Morphology and properties of mixed anion ionomers

Susan A. Visser* and Stuart L. Cooper†
Department of Chemical Engineering, University of Wisconsin–Madison, Madison, WI 53706, USA
(Received 29 April 1991; revised 25 July 1991; accepted 5 August 1991)

A series of model polyurethane ionomers containing varying concentrations of both sulphonate and carboxylate anions is examined. Tensile testing results demonstrate that the greater acid strength of the sulphonate anions causes the ultimate tensile properties of the ionomer to regularly increase as sulphonate content increases. However, the small-strain moduli of two mixed carboxylate/sulphonate ionomers were shown to vary from the trends predicted from strict acid strength arguments; the two mixed-anion ionomers have higher Young's moduli than the fully sulphonated ionomer. D.s.c., d.m.t.a. and SAXS analysis indicates that the modulus enhancement in the mixed-anion ionomer arises from a combination of factors, including aggregate packing, ability to immobilize non-ionic chain segments (ionic anchoring) and degree of phase separation. The onset of flow temperature in d.m.t.a. is seen to decrease in parallel with increasing carboxylate content, unlike the tensile properties. Thus, the concept of mixed anion derivatization is shown to fulfil a primary goal in the ionomer field: development of a method to increase ease of processability while retaining strong tensile properties.

(Keywords: ionomer; polyurethane; mixed-anion type; small-angle X-ray scattering; physical properties)

INTRODUCTION

In previous studies of model polyurethane ionomers, the influence of pendant-anion type on ionomer morphology and properties was examined in detail[1,2]. These studies uncovered the two key factors governing the effect of the pendant anion: (1) the strength of the individual physical crosslinks formed by the anions, as reflected by their relative acid strengths; and (2) the geometrical packing constraints or coordination tendencies of pendant anions, which govern the size of the ionic aggregates. The combined effects of these factors gave the unexpectedly high tensile moduli of the carboxylated ionomers compared to their sulphonated analogues. The high moduli resulted from the larger size of the ionic aggregates in the carboxylated ionomers. This in turn arose from the planar nature of the carboxylate anion[3], with its single coordination distance, which permitted packing arrangements more favourable to formation of larger ionic aggregates.

The weaker character of the individual physical crosslinks in the carboxylated ionomers also gave rise to other effects[1,2]. First, while the Young's moduli of the carboxylated ionomers were higher than expected, their ultimate tensile properties were significantly lower than those of their sulphonated analogues. The lower ultimate properties of the carboxylated ionomers reduces their desirability for use as high-strength, high-toughness elastomers. In addition, as the temperature was increased in the dynamic mechanical experiment[1], the carboxylated ionomers began to flow at markedly lower temperatures than their sulphonated analogues. This lower flow temperature is a very attractive feature if polymer processability is a concern, as it implies a significantly lower heating requirement in the processing and flow stages.

One final and potentially very attractive feature of the carboxylated ionomers was noted which was absent in the sulphonated ionomers. The carboxylated PTMO-based ionomers were insoluble in nearly every solvent tested, including water, acetone, dimethylacetamide, methyl ethyl ketone, toluene and methanol[4]. In contrast, the sulphonated PTMO-based ionomers were soluble in acetone, dimethylacetamide, methyl ethyl ketone and methanol, and they formed emulsions in water[4]. These observations are not surprising, as an enhanced sensitivity of sulphonated ionomers to certain solvents has been observed in a study of carboxylated and sulphonated polystyrene ionomers[5]. As solvent-resistant polymers are extremely useful, an ionomer system that can capitalize on this feature could be very important.

Therefore, in an attempt to combine the strength of the sulphonated ionomers with the processability and chemical resistance of the carboxylated ionomers, a series of model polyurethane ionomers containing both sulphonate and carboxylate groups was prepared. The morphology and properties of the mixed-anion ionomers are examined.

*Present address: Eastman Kodak Company Research Laboratories, Rochester, NY 14650, USA
†Author to whom correspondence should be addressed

0032-3861/92/1833790-07

EXPERIMENTAL

Sample preparation

The synthesis of the model polyurethanes was performed as described[1]. The model polyurethane ionomers are 1:1 copolymers of poly(tetramethylene oxide), (PTMO), $M_n = 990$ (Quaker Oats Polymeg), and tolylene diisocyanate (TDI) (Aldrich Chemical Company), which have propyl sulphonate and/or ethyl carboxylate groups grafted at the urethane linkages. The chemical structure of the ionomers is shown in *Figure 1*. The grafting reactions were carried out as described previously[1], with the following modifications for the mixed-anion ionomers. For the mixed anion ionomers, the γ-propane sultone was added first, and after 10–15 min at ~0°C, the β-propiolactone was added. After reaction for two hours, the ionomer was recovered by precipitation into an appropriate non-solvent. Structures were verified by Fourier transform infrared spectroscopy (*FT*i.r.) and by atomic absorption analysis (Galbraith Laboratories).

Samples for tensile testing and further physical analysis were compression moulded because the solvent resistance of the carboxylate-containing ionomers made impossible the selection of an experimentally tractable solvent for all the ionomers. Apparently, the solvent resistance of the fully carboxylated ionomers also carries over into the mixed-anion systems. Samples were compression moulded at 160°C for 5 min at 10000 psi (~69 MPa) and allowed to slowly cool to room temperature in the mould over the period of one hour.

Instrumental conditions

Dogbone samples for uniaxial stress–strain testing were stamped out with a standard ASTM D1708 die and were tested by using an Instron TM model at room temperature in air, with a crosshead speed of 0.5″ min^{-1} (~1.27 cm min^{-1}). Differential scanning calorimetry (d.s.c.) thermograms were recorded with a Perkin-Elmer DSC-7. Sample weights were 11 ± 2 mg. Thermograms were recorded from −130 to 150°C at a heating rate of 20°C min^{-1}. Dynamic mechanical thermal analysis (d.m.t.a.) data were obtained by using a Rheometrics RSA-II at a test frequency of 100 rad s^{-1} (15.9 Hz) under a dry nitrogen purge. Temperature steps of 3°C per step were used, with 0.1 min equilibration time at each step.

SAXS measurements

The small-angle X-ray scattering (SAXS) data were obtained with an Elliot GX-21 rotating anode generator, an Anton-Paar compact Kratky scattering camera and a Braun linear position-sensitive detector. CuKα radiation was monochromatized by using a nickel filter and pulse-height discrimination. The scattering camera

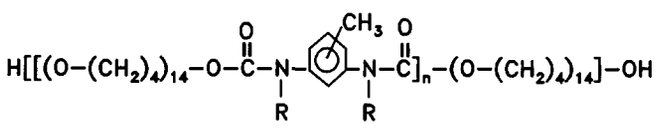

R = $-(CH_2)_3-SO_3Na^+$ or $-(CH_2)_2CO_2Na^+$

Figure 1 Structure of model polyurethane ionomer: n is the overall degree of polymerization

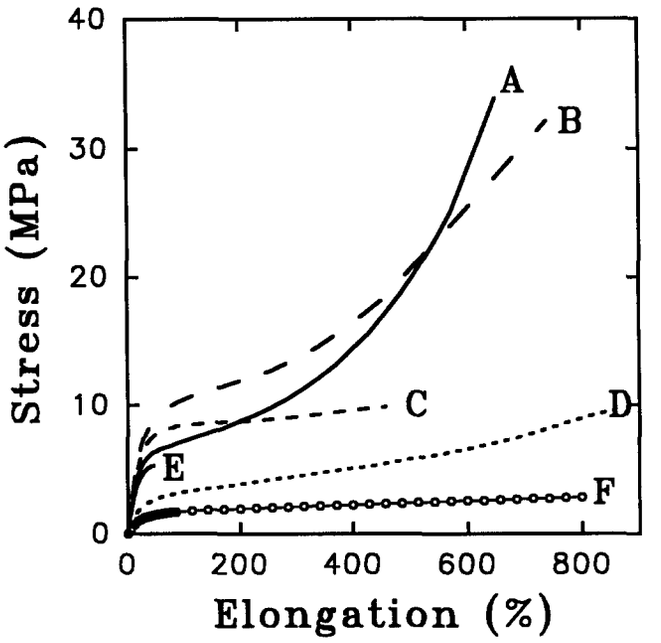

Figure 2 Uniaxial stress–strain results for single- and mixed-anion ionomers: (A) M1SC93/0; (B) M1SC73/13; (C) M1SC54/41; (D) M1SC23/67; (E) M1SC0/98; (F) M1SC0/57

has a sample–detector distance of 60 cm and a detector length of approximately 8 cm. This configuration allowed a q ($q = (4\pi/\lambda)(\sin\theta)$, where 2θ is the scattering angle and λ is the wavelength of the radiation) range of 5.7 nm^{-1}, with a minimum q of 0.15 nm^{-1} due to the position of the beam stop, to be probed. The detector length was divided into 128 channels for a resolution of ~0.05 nm^{-1}. All data were collected at room temperature.

The data were corrected for detector sensitivity, parasitic and background scattering and absorption of X-rays by the sample. The beam profile along the slit length was measured and the iterative method developed by Lake[6] was used to desmear the data. Absolute intensities expressed in terms of I/I_eV, where I_e is the intensity scattered by a single electron and V is the scattering volume, were determined by comparing the sample scattering intensity to that from a calibrated Lupolen (polyethylene) standard[7]. Background scattering was determined by fitting the SAXS data in the high q region by using Porod's law[8] plus a constant-background term.

Sample nomenclature

The first four characters of the code (M1SC) indicate PTMO(1000)/TDI ionomers containing propyl sulphonate and ethyl carboxylate groups at the urethane linkages. The number immediately following indicates the percentage of urethane nitrogens that contain propyl sulphonate grafts. The number following the solidus (/) indicates the percentage of urethane nitrogens with ethyl carboxylate grafts. All ionic groups in these polymers are neutralized with a stoichiometric amount of sodium cation.

RESULTS AND DISCUSSION

Tensile testing

Uniaxial stress–strain results for the series of mixed-anion ionomers are shown in *Figure 2*. Young's moduli (E_0) and stress (σ_b) and strain (ε_b) at break for

Table 1 Tensile properties of mixed-anion ionomers

Sample	Percentage[a] substitution ($\%SO_3/\%CO_2$)	E_0[b] (MPa)	Stress at break, σ_b (MPa)	Elongation at break (%)	Mooney–Rivlin results, α_c
M1SC93/0	93/0	36.4	33.9	650	5.0
M1SC73/13	73/13	43.3	32.1	740	5.0
M1SC54/41	54/41	40.4	9.9	460	–
M1SC23/67	23/67	12.9	9.6	860	–
M1SC0/98	0/98	29.0	5.3	46	–
M1SC0/57	0/57	6.5	2.9	810	–

[a]From elemental analysis for sulphur, for sulphonate groups, or for sodium, for carboxylate groups
[b]Zero-strain Young's modulus from slope of stress–strain curve at $\leqslant 5\%$ elongation

each material are shown in *Table 1*. As expected[1,9–15], the greater acid strength of the sulphonate anions gave rise to stronger physical crosslinks at the higher elongations. Thus, the stress at break decreased as the sulphonate content decreased in the order

$$\text{M1SC93/0} > \text{M1SC73/13} > \text{M1SC54/41} > \text{M1SC23/67} > \text{M1SC0/98}$$

Strain-hardening behaviour, observed in a number of other model polyurethane ionomer systems[1,16,17], is observed for M1SC93/0 and M1SC73/13, but not for any of the higher carboxylate-content ionomers. Strain-hardening behaviour probably results from strain-induced crystallization, as has been observed in other PTMO-based polyurethanes by wide-angle X-ray scattering (WAXS)[18]. The absence of strain-hardening in the higher carboxylate-content ionomers is probably an indication that the critical carboxylate content has been reached. A critical carboxylate content for stress crystallization inhibition was observed previously for single-anion carboxylate ionomers[1]. Below the critical carboxylate content, differences between sulphonated and carboxylated ionomers were nearly indistinguishable and both sulphonated and carboxylated ionomers exhibited strain-hardening. Above the critical ion content, the carboxylated ionomers no longer gave the upturn in the stress–strain curve that characterizes strain-hardening. The importance of a critical ion content in predicting ionomer properties has been stressed in a number of other studies as well[5,17,19–21], lending credence to this argument.

One possible explanation for the observation of a critical ion content for carboxylated but not sulphonated ionomers in stress–strain tests is that the sulphonate groups disturb the crystalline matrix less than the carboxylate groups[22]. Another possible explanation recalls the dynamic nature of the stress–strain test. As the ionomer is elongated, the ionic aggregates can rearrange without wholesale dissociation through the process of ion-hopping[23–25]. Ion hopping allows relaxation of the polyol chains, delaying the onset of stress crystallization. This suggests that ion-hopping is easiest in the weaker materials, M1SC54/41, M1SC23/67 and M1SC0/98, and most difficult in M1SC93/0 and M1SC73/13, exactly as predicted based on arguments of acid strength of the pendant anions. Evidence for the ion-hopping explanation appears in the flow temperatures measured with d.m.t.a., discussed below. The d.m.t.a. results show that the temperature at which flow begins decreases as carboxylate content increases, indicating that physical crosslink cohesiveness decreases and ease of ion-hopping increases similarly.

The effect of adding a small amount of sulphonate anion to a partially carboxylated ionomer is easily discerned when the stress–strain curves of M1SC0/57 and M1SC23/67 are compared. Addition of the small fraction of sulphonate anions dramatically increases the Young's modulus and stress at break, while only inducing a slight decrease in elongation at break. In contrast, comparing the results for M1SC0/98 to M1SC23/67 indicates that adding a similar amount of carboxylate anion gives significantly lower modulus and stress at break and greatly reduces the strain at break. The advantages inherent in the mixed-anion system are apparent.

Unlike the ultimate tensile properties, the small-strain tensile modulus (E_0) does not follow the trend predicted solely on acid strength arguments. In order to illustrate the trend in initial moduli observed here, the stress–strain data were recast in the Mooney–Rivlin format[26,27]:

$$[f] = \frac{\sigma}{(\alpha - 1/\alpha^2)} \tag{1}$$

where $[f]$ is termed the reduced stress, σ is the engineering stress and α is the ratio of the stressed to unstressed sample length. For low elongations, where the time-dependent nature of the physical crosslinks affects the data least[28], the small-strain tensile modulus is directly proportional to the $1/\alpha = 1$ intercept of the Mooney–Rivlin curves. The Mooney–Rivlin plots for the fully substituted ionomers are shown in *Figure 3*.

Figure 3 clearly illustrates the decrease of the small-strain moduli in the order M1SC73/13 > M1SC54/41 > M1SC93/0 > M1SC0/98 > M1SC23/67. A number of factors that contribute to this ordering are discussed below. The Mooney–Rivlin format also allows determination of the elongation at which strain-hardening begins, denoted as α_c. Evidence for strain-hardening is provided by the positive deviation from linearity at low values of $1/\alpha$ on the Mooney–Rivlin plots for M1SC93/0 and M1SC73/13. As was seen previously for single-anion polyurethane ionomers exhibiting strain-hardening behaviour[1], the onset of strain-hardening is independent of anion type. The data here show that α_c is also unaffected by the mixture of the two anion types. This implies that the onset of strain-induced crystallization is governed primarily by the type and concentration of the ionic groups rather than by their local packing arrangements, which undoubtedly differ between the single-anion and mixed-anion ionomers.

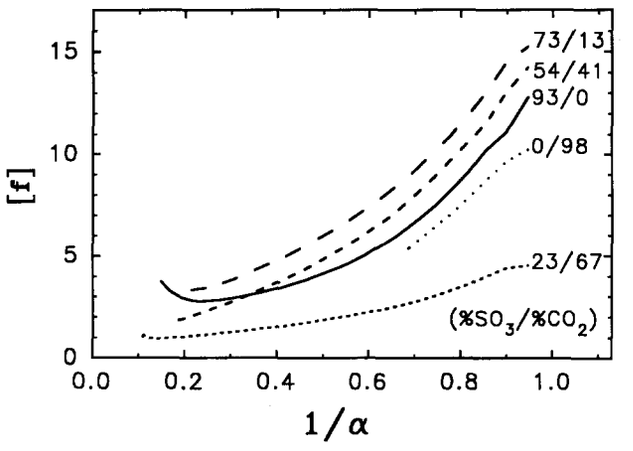

Figure 3 Mooney–Rivlin plots for fully substituted single- and mixed-anion model polyurethane ionomers: numbers to the right of each curve indicate the percentage of propyl sulphonate and ethyl carboxylate groups substituted at the urethane linkages

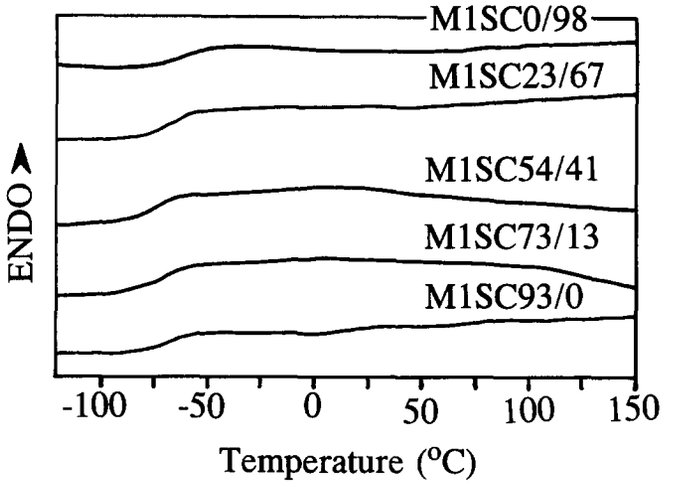

Figure 4 D.s.c. thermograms for the single- and mixed-anion model polyurethane ionomers

Differential scanning calorimetry

One factor that may make a strong contribution to the unusual stress–strain properties of the mixed-anion ionomers is the degree of phase separation. D.s.c. was used to probe the degree of phase separation in the ionomers. D.s.c. thermograms for the mixed-anion ionomer series are shown in *Figure 4*, and the d.s.c. data are summarized in *Table 2*. All ionomers examined exhibited only a well-defined glass transition, the mid-point of which is reported as the glass transition temperature, T_g, in *Table 2*.

The T_gs of M1SC93/0, M1SC73/13 and M1SC23/67 are essentially identical within experimental error (±2°C). In contrast, the T_g of M1SC54/41 is lower, approaching the T_g of the pure PTMO polyol (−84°C)[29]. At −75.4°C, the measured T_g of M1SC54/41 is indistinguishable from the measured T_g of M1SC93/0 (−72.1°C) within experimental error, but it is significantly lower than the T_gs of the other mixed-anion ionomers. Since the T_g is primarily determined by the T_g of the PTMO soft segment and the purity of the soft-segment phase[1,30], the lower T_g of M1SC54/41 indicates a higher degree of phase separation in this ionomer than in the other mixed-anion ionomers.

As has been noted for solution-cast carboxylated polyurethane ionomers[1], the T_g of the fully carboxylated ionomer M1SC0/98 is much greater than the T_gs of the sulphonate-containing ionomers, indicating a lower degree of phase separation in M1SC0/98. The phase-mixed morphology of M1SC0/98 rationalizes its relatively low tensile properties.

Dynamic mechanical thermal analysis

In order to further explore the thermal and mechanical behaviour of the mixed-anion ionomers, d.m.t.a. was performed. The storage moduli (E') and loss tangents (tan δ) are plotted as a function of temperature in *Figures 5* and *6*, and the d.m.t.a. results are summarized in *Table 3*. The T_gs are taken as the maxima in the loss moduli (data not shown).

Table 2 D.s.c. results for mixed-anion ionomers

Sample	T_g (°C)
M1SC93/0	−72.1
M1SC73/13	−70.4
M1SC54/41	−75.4
M1SC23/67	−68.2
M1SC0/98	−64.5

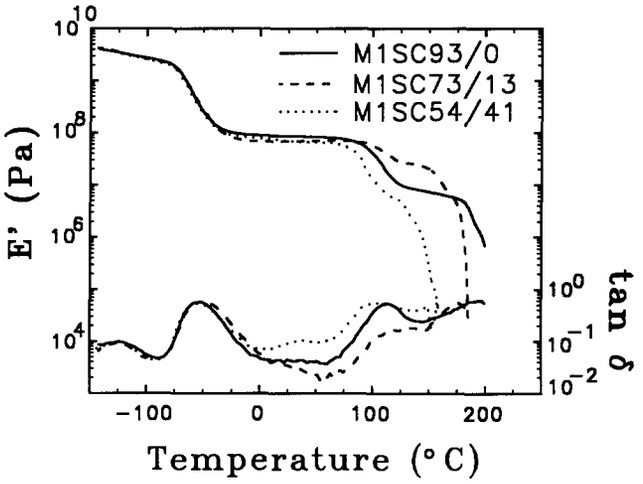

Figure 5 D.m.t.a. results, E' and tan δ, for the first three ionomers in the mixed-anion ionomer series

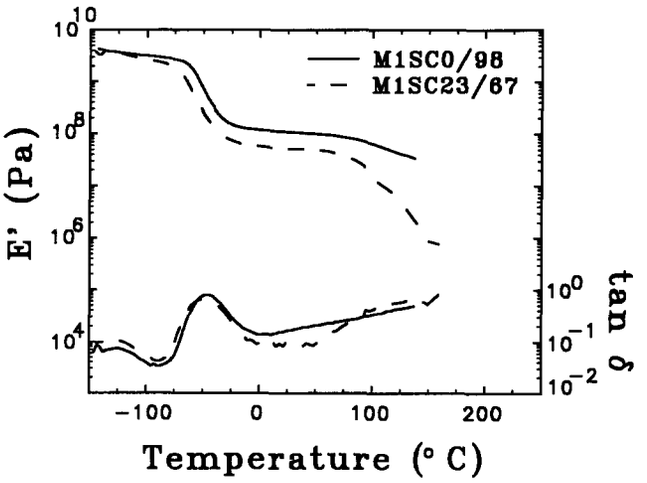

Figure 6 D.m.t.a. results, E' and tan δ, for the remaining two ionomers in the mixed-anion ionomer series

Table 3 D.m.t.a. results for mixed-anion ionomers

Sample	T_g (°C)	High T transition (°C)	Onset of flow (°C)
M1SC93/0	−66	99	181
M1SC73/13	−66	106	172
M1SC54/41	−68	86	127
M1SC23/67	−65	81	106
M1SC0/98	−56	(77)[a]	(77)[a]

[a]Because of physical failure of the ionomer samples at higher temperatures, it could not be determined if this was the high-temperature transition seen in the other mixed anion ionomers or if this temperature represented the onset of flow

While the differing scan rates of the d.s.c. (20°C min^{-1}) and d.m.t.a. (15.9 Hz) experiments cause their timescales to differ[31] and hence shift transition values, there is qualitative agreement between the trends in T_g observed by d.s.c. and by d.m.t.a. The M1SC93/0, M1SC73/13 and M1SC23/67 ionomers exhibit essentially identical T_gs in the d.m.t.a. experiments. Again, the T_g of M1SC54/41 appears to be lower than the T_gs of the other mixed-anion ionomers, but no definitive conclusions can be drawn because the differences are within experimental error. In contrast, the T_g of M1SC0/98 is significantly higher. The implications of these results were discussed above.

The physical crosslinking of the ionic groups in the polyurethane ionomers gives rise to an extended rubbery plateau, as has been observed in many ionomer systems[1,16,32,33]. In addition, higher temperature relaxations are observed for all the sulphonate-containing ionomers. Higher temperature ionic relaxations have been observed in a number of ionomer systems[34–37], where they were ascribed to 'ionic transitions' of unspecified nature. More recently, the relaxations have been described as T_gs of the ionic aggregates[38,39]. However, the failure to detect these transitions in the d.s.c. data raises some concern. It is also unclear if the ionic aggregates extend over areas great enough to generate a clear ionic microphase T_g. If it is assumed instead that the temperature of the ionic transitions is governed by the ability of the ionic groups to limit the motion of the attached polymer chain in the immediate vicinity of ionic groups (not just the aggregates), as suggested by Eisenberg's new model of ionomer morphology[40], then it can be said that the greatest immobilization, or 'ionic anchoring', occurs in M1SC73/13, which has the highest temperature ionic transition. This explanation does not require ionic aggregates of a size that could give rise to a distinct ionic T_g and correlates well with the high tensile modulus of M1SC73/13.

The downturn in the E' *versus* temperature curves indicates the onset of flow and the failure of the ionic aggregates as physical crosslinks. The temperature at which the onset of flow occurs is indicative of the strength of the physical crosslinks and decreases in the order M1SC93/0 > M1SC73/13 > M1SC54/41 > M1SC23/67. The onset of flow could not be determined unambiguously for M1SC0/98 because of catastrophic failure of the material at higher test temperatures. The trend observed for the onset of flow confirms the arguments presented throughout this study regarding physical crosslink strength: sulphonate groups form stronger physical crosslinks and the more sulphonate groups in an ionomer, the greater is the ultimate strength of the crosslinks. These data also indicate that ionomer processability, or the heat input necessary for processing, is directly correlated to the carboxylate content. If a constant overall level of ionic substitution is maintained, adding more carboxylate groups proportionately lowers the flow temperature and therefore increases the processability.

Small-angle X-ray scattering

The SAXS patterns for the mixed-anion ionomers appear in *Figures 7* and *8*. The scattering patterns show

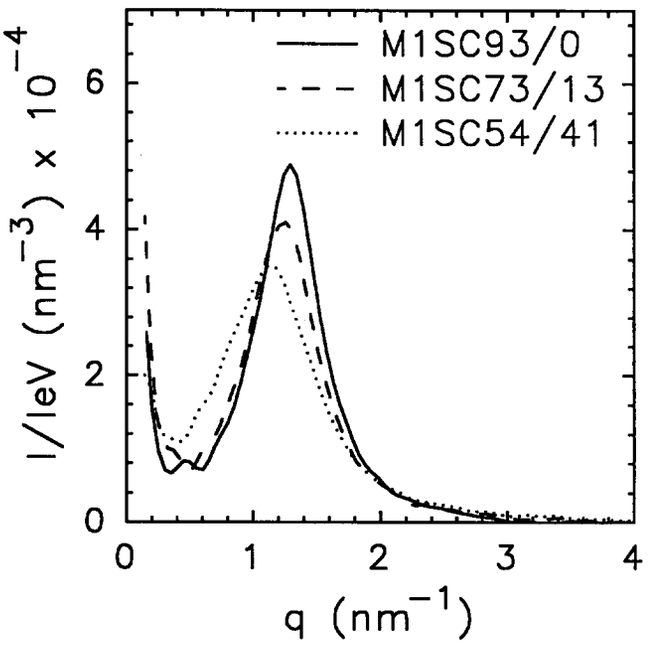

Figure 7 SAXS patterns for the first three ionomers in the mixed-anion ionomer series

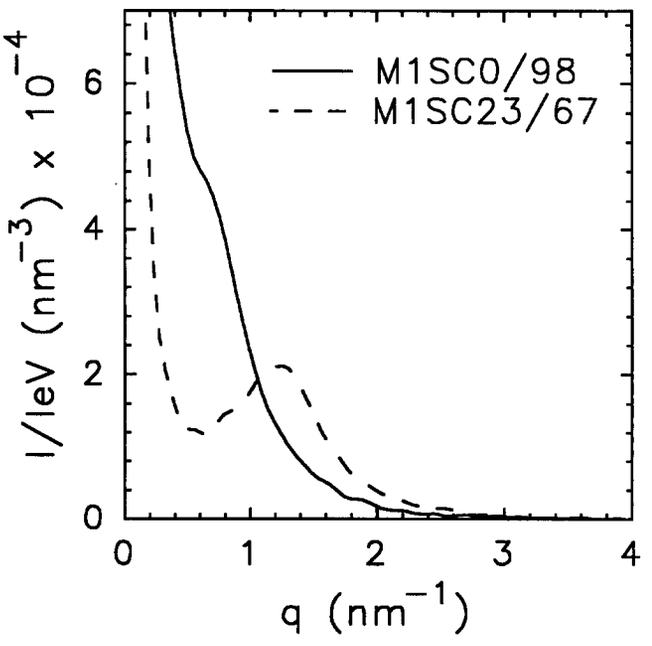

Figure 8 SAXS patterns for the final two ionomers in the mixed-anion ionomer series

the two features typical of ionomer SAXS data[2,41,42]: an upturn in intensity at low scattering vector, q, which has been attributed to an inhomogeneous distribution of ionic groups[43,44]; and a peak or shoulder on the upturn, which is indicative of ionic aggregation and is usually referred to as the 'ionomer peak'.

To quantitatively analyse the data, they were fitted to the modified liquid-like interparticle interference model described previously[2]. The model[45] envisages the ionic aggregates to be hard spheres of electron density ρ_1 and radius R_1, which are surrounded by a corona of polymer chain of radius R_2 ($R_2 > R_1$) and electron density ρ_0, equal to the electron density of the matrix. The ionic spheres are distributed in the polymer matrix with a liquid-like degree of order; the Percus–Yevick total correlation function[46–48] describes the interparticle scattering interactions that give rise to the scattering peak. An evaluation of this model has confirmed its usefulness in modelling SAXS data from model polyurethane ionomers[2]. The model has four fitting parameters: the two radii R_1 and R_2; the electron density difference between the aggregates and the matrix $\Delta\rho = \rho_1 - \rho_0$; and v_p, the volume of material per ionic aggregate. The model-fitted results are given in *Table 4*.

The data for M1SC0/98 were not modelled because of the uncertainty inherent in deconvolution of the upturn and the ionic shoulder. Nevertheless, comparison of the shoulder position with the peak positions of the sulphonate-containing ionomers confirms the larger size of the carboxylate ionic aggregates and correspondingly lower degree of phase separation, as observed in the d.s.c. and d.m.t.a. data.

Comparison of the ionic core radii (R_1) for the four ionomers listed in *Table 4* shows that R_1 remains constant for sulphonate-containing ionomers. The R_2 values also remain essentially unchanged as anion content is varied. When the widely differing SAXS data for M1SC0/98 are considered, the constancy of the radii in the sulphonate-containing ionomers suggests that the ionic core and sheath radii are determined predominantly by the sulphonate anion.

The $\Delta\rho$ and v_p values vary as the anion type and content are changed. If the matrix is assumed to consist predominantly of PTMO, an estimate of the aggregate electron densities can be calculated. By using a density value of 0.98 g cm^{-3} for PTMO[49], the electron density of the matrix, ρ_0 is calculated to be 327 e nm^{-3}. In combination with the electron density differences ($\Delta\rho$) obtained from the model, the aggregate electron densities ρ_1 shown in *Table 4* are derived. The aggregate electron densities decrease in the order M1SC54/41 > M1SC73/13 > M1SC93/0 > M1SC23/67, reflecting a decrease in ionic packing densities in the same order. The greater ionic packing density in M1SC54/41 compared to M1SC93/0 correlates with the higher degree of phase separation in M1SC54/41 observed in d.s.c. and d.m.t.a. data and rationalizes the higher small-strain modulus of M1SC54/41. While the carboxylate anions form slightly weaker physical crosslinks than the sulphonate anions, the higher packing densities imply that more ionic groups are present in the M1SC54/41 aggregates to produce the higher initial modulus. The low ρ_1 value of M1SC23/67, even when the lower electron density of the carboxylate compared to the sulphonate anions is considered, similarly correlates with the lower tensile modulus of M1SC23/67.

Table 4 Small-angle X-ray scattering model parameters

Sample	R_1 (nm)	R_2 (nm)	v_p (nm^3)	$\Delta\rho$ (nm^{-3})	ρ_1 (nm^{-3})
M1SC98/0	1.56	2.36	172	227	554
M1SC73/13	1.54	2.42	202	233	560
M1SC54/41	1.55	2.42	278	254	581
M1SC23/67	1.52	2.25	216	192	519

Consideration of the v_p values (the inverses of the aggregate number densities) reveals complications inherent in analyses of these systems. Presumably, ionomers with the highest aggregate number densities should have the highest tensile moduli, assuming all other factors are equal. Yet, the aggregate number densities decrease in the order M1SC98/0 > M1SC73/13 > M1SC23/67 > M1SC54/41, displaying little or no correlation with the trends observed for the tensile moduli. The higher number density of ionic aggregates in M1SC73/13 compared to M1SC54/41 and M1SC23/67 correlates with the tensile modulus trends, yet the low aggregate number density of M1SC54/41 demonstrates that a number of other factors must be working in concert to enhance its tensile modulus.

CONCLUSIONS

A series of model polyurethane ionomers containing various amounts of sulphonate and carboxylate anions was examined. In tensile testing, the stress and strain at break varied exactly as predicted based on acid strength arguments. However, the combination of the sulphonate and carboxylate anions gave unexpected small-strain results for two ionomers: M1SC73/13 and M1SC54/41. Both exhibited Young's moduli in excess of that of the completely sulphonated ionomer M1SC93/0. This was attributed to the greater aggregate packing densities, corresponding to a greater number of ionic groups per aggregate, in M1SC73/13 and M1SC54/41 and to the greater ionic anchoring in M1SC73/13 and the increased phase separation in M1SC54/41. The enhanced tensile properties in these ionomers are additional bonuses of the mixed ionomer system compared to the conventional single-anion-type ionomer. The need to consider the strength of the individual carboxylate and sulphonate anions as physical crosslinks, along with the aggregate packing, ionic microphase anchoring of non-ionic chain segments and phase-separation factors was emphasized when comparing the small-strain behaviour of M1SC73/13 and M1SC54/41.

The incorporation of a small fraction of carboxylate anion in a sulphonated ionomer was shown by d.m.t.a. to increase processability by lowering flow temperatures, without greatly reducing the tensile properties. This directly addresses one of the primary goals of ionomer design: to develop an ionomer system that retains high tensile strength while providing for ease in melt processing. In some systems where processability was an issue, processability was enhanced by addition of an ionic plasticizer (see, for example, the discussion in reference 50) at the cost of decreased tensile properties. The suggestion of the mixed-anion concept for ionomers, therefore, represents a definite step forward in the development of new-generation ionomers.

ACKNOWLEDGEMENTS

Support for this work was provided by the US Department of Energy through Grant DE-FG02-88ER45370; by the donors of the Petroleum Research Fund, administered by the American Chemical Society, through Grant 20343-AC7. SAV gratefully acknowledges the fellowship support of the American Association of Women Educational Fund in the form of an Engineering Dissertation Fellowship.

REFERENCES

1 Visser, S. A. and Cooper, S. L. *Macromolecules* 1991, **24**, 2576
2 Visser, S. A. and Cooper, S. L. *Macromolecules* 1991, **24**, 2584
3 Wells, A. F. 'Structural Inorganic Chemistry', 5th Edn, Oxford University Press, New York, 1984
4 Visser, S. A. Unpublished results
5 Lundberg, R. D. and Makowski, H. S. 'Ions in Polymers' (Ed. A. Eisenberg), ACS Symp. Ser. 187, American Chemical Society, Washington, DC, 1980, p. 21
6 Lake, J. A. *Acta Crystallogr.* 1967, **23**, 191
7 Kratky, O., Pilz, I. and Schmitz, P. J. *J. Colloid Interface Sci.* 1966, **21**, 24
8 Porod, G. *Kolloid Z.* 1951, **124**, 83
9 Hashimoto, T., Fujimura, M. and Kawai, H. 'Perfluorinated Ionomer Membranes' (Eds A. Eisenberg and H. L. Yeager) ACS Symp. Ser. 180, American Chemical Society, Washington, DC, 1982, p. 217
10 Rahrig, D., Azuma, C. and MacKnight, W. J. *J. Polym. Sci., Polym. Phys. Edn.* 1978, **16**, 59
11 Rahrig, D., MacKnight, W. J. and Lenz, R. W. *Macromolecules* 1979, **12**, 195
12 Rahrig, D. and MacKnight, W. J. 'Ions in Polymers' (Ed. A. Eisenberg), ACS Symp. Ser. 187, American Chemical Society, Washington, DC, 1980, p. 91
13 Rahrig, D. and MacKnight, W. J. 'Ions in Polymers' (Ed. A. Eisenberg), ACS Symp. Ser. 187, American Chemical Society, Washington, DC, 1980, p. 77
14 Sanui, K. and MacKnight, W. J. *Brit. Polym. J.* 1974, **8**, 22
15 Sanui, K., Lenz, R. and MacKnight, W. J. *J. Polym. Sci., Polym. Chem. Edn* 1974, **12**, 1965
16 Ding, Y. S., Register, R. A., Yang, C. Z. and Cooper, S. L. *Polymer* 1989, **30**, 1204
17 Lee, D. C., Register, R. A., Yang, C. Z. and Cooper, S. L. *Macromolecules* 1988, **21**, 1005
18 Clough, S. B. and Schneider, N. *J. Macromol. Sci., Phys.* 1968, **2**, 553
19 Mattera, V. D. Jr and Risen, W. M. *J. Polym. Sci., Polym. Phys. Edn.* 1986, **24**, 753
20 Eisenberg, A. and Navratil, M. *Macromolecules* 1973, **6**, 604
21 Eisenberg, A. and Navratil, M. *Macromolecules* 1973, **6**, 734
22 Rahrig, D., MacKnight, W. J. and Lenz, R. W. *Macromolecules* 1979, **12**, 195
23 Ward, T. C. and Tobolsky, A. V. *J. Appl. Polym. Sci.* 1967, **11**, 2403
24 Sakamoto, K., MacKnight, W. J. and Porter, R. S. *J. Polym. Sci., A-2* 1970, **8**, 277
25 Hara, M., Eisenberg, A., Storey, R. F. and Kennedy, J. P. 'Coulombic Interactions in Macromolecular Systems' (Eds A. Eisenberg and F. E. Bailey), ACS Symp. Ser. 302, American Chemical Society, Washington, DC, 1986, p. 176
26 Mooney, M. *J. Appl. Phys.* 1940, **11**, 582
27 Rivlin, R. *Phil. Trans. R. Soc. London. Ser. A* 1948, **241**, 379
28 Register, R. A., Foucart, M., Jerome, R., Ding, Y. S. and Cooper, S. L. *Macromolecules* 1988, **21**, 1009; correction 1988, **21**, 2652
29 Brandrup, J. and Immergut, E. (Eds) 'Polymer Handbook', 2nd Edn, Wiley, New York, 1975, pp. 11–157
30 Visser, S. A. and Cooper, S. L. *Polymer* 1992, **33**, 920
31 Sperling, L. H. 'Introduction to Physical Polymer Science', Wiley, New York, 1986
32 Lundberg, R. D. 'Structure and Properties of Ionomers' (Eds M. Pineri and A. Eisenberg), D. Reidel Publishing Company, Boston, 1987, p. 429
33 Gauthier, M. and Eisenberg, A. *Macromolecules* 1989, **22**, 3754
34 Fitzgerald, J. J., Kim, D. and Weiss, R. A. *J. Polym. Sci., Polym. Lett. Edn* 1986, **24**, 263
35 Bazuin, C. G. and Eisenberg, A. *J. Polym. Sci., Polym. Phys. Edn.* 1986, **24**, 1137
36 Bazuin, C. G., Eisenberg, A. and Kamal, M. *J. Polym. Sci., Polym. Phys. Edn.* 1986, **24**, 1155
37 Eisenberg, A. and Navratil, M. *Macromolecules* 1974, **7**, 90
38 Villeneuve, S. and Bazuin, C. G. *Polymer* **32**, 2811
39 Hird, B. and Eisenberg, A. *J. Polym. Sci., Polym. Phys. Edn.* 1990, **28**, 1665
40 Eisenberg, A., Hird, B. and Moore, R. B. *Macromolecules* 1990, **23**, 4098
41 Ding, Y. S., Register, R. A., Yang, C. Z. and Cooper, S. L. *Polymer* 1989, **30**, 1213
42 MacKnight, W. J., Taggart, W. P. and Stein, R. S. *Macromol. Sci., Rev. Macromol. Chem.* 1981, **16**, 41
43 Register, R. A. and Cooper, S. L. *Macromolecules* 1990, **23**, 310
44 Register, R. A. and Cooper, S. L. *Macromolecules* 1990, **23**, 318
45 Yarusso, D. J. and Cooper, S. L. *Macromolecules* 1983, **16**, 1871
46 Percus, J. K. and Yevick, G. *Phys. Rev.* 1958, **110**, 1
47 Wertheim, M. S. *Phys. Rev. Lett.* 1963, **10**, 321
48 Thiele, E. *J. Chem. Phys.* 1963, **39**, 474
49 Miller, R. L. 'Polymer Handbook', 3rd Edn (Eds J. Brandrup and E. H. Immergut), John Wiley and Sons, New York, 1989, p. IV–72
50 Jackson, D. A., Weiss, R. A. and Koberstein, J. T. *ACS Div. Polym. Chem. Prepr.* 1991, **32**(1), 120